



Calibration of pneumatic multi-hole probes for transonic turbomachinery flows

Johannes R. Bachner¹ · Andreas Pahs¹ · Philipp Weggler¹ · Frank Kocian¹ · Marcel Rößling²

Received: 28 February 2022 / Revised: 15 July 2022 / Accepted: 27 July 2022
© The Author(s) 2022

Abstract

The calibration data of a five-hole probe and a six-hole probe designed for measurements in transonic turbomachinery flows are presented. The probes feature a special base pressure hole on the back side to avoid the Mach number insensitivity of pressure probes near Mach number unity. There is only little literature available on the performance of such probes, especially in flows with large radial flow angles. To close this gap, the probes are calibrated for radial flow angles up to 32° . A significant influence of this flow angle on the coefficients used for Mach number determination is shown. At large positive flow angles, the relationship between the pressure coefficient using the base pressure and the Mach number is not biunique for the six-hole probe. Therefore, an experimental study of Mach number measurement deviations is performed at the calibration wind tunnel. Different evaluation methods are examined. The sample standard deviation over 210 randomly distributed points is reduced by 66% compared to the same probe design without the base pressure hole. This is achieved using two calibration coefficients for the Mach number simultaneously in a multidimensional interpolation.

Keywords Five-hole probe · Pneumatic probe · Transonic flow measurement · Turbomachinery measurement

List of symbols

α	Yaw angle with respect to probe
β	Pitch angle with respect to probe
C_α, C_β	Pressure coefficients for flow angles
C_{Ma}, C_{Mab}	Pressure coefficients for Mach number
C_{MaX}	Simultaneous use of C_{Ma} and C_{Mab}
$E(Ma)$	Measurement deviation of Mach number
$ E(Ma) _{max}$	Maximum absolute value of $E(Ma)$
κ	Isentropic coefficient
Ma	Mach number
Ma_{probe}	Mach number measured by probe
Ma_{ref}	Reference Mach number
$m(C_{Ma}), m(C_{Mab})$	Slopes of pressure coefficients
p_1, p_2	Calibration points for calculating slopes of coefficients
P_C	Probe center pressure
P_L	Probe left pressure

P_R	Probe right pressure
P_D	Probe down pressure
P_B	Probe base pressure
P_T	Probe top pressure
P_m	Mean pressure for either 5HP or 6HP
$P_{m,5HP}$	Mean pressure as defined for 5HP
$P_{m,6HP}$	Mean pressure as defined for 6HP
Re	Reynolds number
σ	Sample standard deviation

Abbreviations

5HP	Five-hole probe
6HP	Six-hole probe
DLR	German Aerospace Center
PIV	Particle image velocimetry
SKG, SEG	Probe calibration facility Göttingen
SLM	Selective laser melting
TC	Thermocouple

✉ Johannes R. Bachner
johannes.bachner@dlr.de

¹ Institute for Propulsion Technology, German Aerospace Center (DLR), 37073 Göttingen, Germany

² Engineering Systems House, German Aerospace Center (DLR), 37073 Göttingen, Germany

1 Introduction

To acquire a thorough understanding of the complex flow phenomena in research turbines and for the validation of numerical flow models, experimental data with high accuracy are essential. Pneumatic multi-hole probes are among

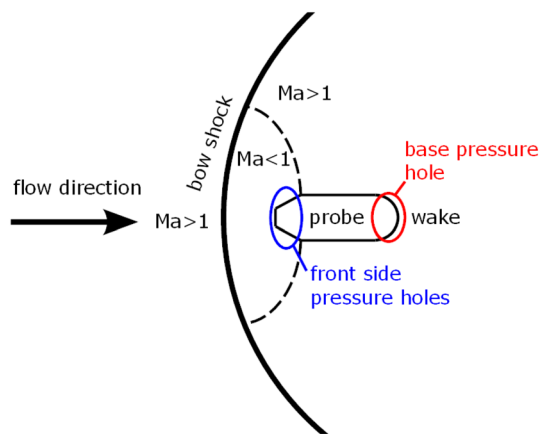


Fig. 1 Bow shock of a conical probe head with the locations of front and base pressure holes

the most widely used measurement instruments for these applications. Equipped with a thermocouple, these allow the determination of the complete thermodynamic state of the flow. However, aligning the probes with the radial flow angle is usually not possible given the tight space constraints in research turbines. Moreover, even small production-related geometrical irregularities between probes influence the probe behavior. Therefore, probe calibration in a known flow field is necessary prior to the measurements. Hence, the relationship between the directly measured pressures and temperatures and other flow properties, such as the Mach number Ma , is determined for each probe [1, 2].

To obtain accurate total pressures and temperatures, it is important to correct directly measured pressures and temperatures with Mach number dependent factors [3]. As a result, accurate measurements not only of flow speed but also of these quantities rely on a precise determination of the Mach number. Thus, it is of particular interest to optimize Mach number determination.

However, determining the Mach number in transonic flows poses a challenge to intrusive, pressure-based measurement instruments such as probes. Fransson [4] noted that measuring the static pressure, crucial for accurate determination of the Mach number, is especially demanding. The supersonic flow field around obstacles is described by Sinclair and Cui [5] as well as Mishra et al. [6]. Due to the obstruction posed by the probe, a shock forms upstream of the probe even at Mach numbers slightly below unity. A sketch of the bow shock of a probe with a conical probe head is shown in Fig. 1. Based on normal shock and isentropic relations, Hancock [7] derived that the pressure near the probe head is independent of Mach number at $Ma = 1$. As the sensitivity increases only gradually for higher and lower Mach numbers, pneumatic probes have low Mach number sensitivity in transonic flows [8–10]. For example, Börner

et al. [11] calculated an increase in the Mach number deviation by a factor of five resulting from a given pressure error when using a multi-hole probe with a hemispherical head in transonic flow.

The source of this issue is the location of the pressure holes, which are typically situated near the probe tip where the shock is approximately normal. Consequently, multiple authors have proposed probe designs with additional pressure holes in regions that are further away from the tip [9, 11, 12]. The Mach number in the flow adjacent to these pressure holes remains supersonic, resulting in an increased probe sensitivity. This approach has led to the development of a wedge probe with pressure holes on the sides of the probe head perpendicular to the flow direction by Amecke [12]. The side holes are deliberately placed on surfaces that are shielded from direct impingement by the flow to reduce dependence of the measured pressures on flow angles. This design was modified and miniaturized by Börner et al. [11] who confirmed its increased sensitivity compared to a hemispherical probe. However, these types of probes with probe heads that are aligned with the shaft are usually unsuited for investigations of turbomachinery components with rotating parts. To access the flow in research turbines, the probes are typically inserted radially into the flow between blade rows. Hence, elbowed probes with probe heads perpendicular to the shaft are used.

Kost [9] designed a probe for transonic flow measurements by equipping a three-hole cobra probe with an additional pressure hole on its back side. The hole opens towards the bottom side of the probe and is cut obliquely for better protection from the flow. This allows measuring the so-called base pressure near the wake of the probe. With the ratio of the pressure at the center hole on the front side to the base pressure, a pseudo-Mach number can be calculated that indicates the Mach number in transonic flow. The general location of the front pressure holes and the base pressure hole are highlighted in Fig. 1.

Continuously changing operating conditions necessitate the constant development of new probes. However, the lack of literature concerned with elbowed probes with base pressure holes makes it difficult to anticipate the exact behavior of such probes. The calibration curves presented by Kost [9] are limited to flow which is directly aligned with the probe head. However, large radial flow angles can occur in turbomachinery flows due to secondary flow phenomena such as purge flows between stationary and rotary parts.

The aim of the current study is to improve the understanding of the behavior of probes with a base pressure hole in flows with radial flow angles. The calibration of two different probes for a wide range of radial angles is presented. The relation between differences in probe behavior and the probe geometries is discussed. Finally, for one of the probes, experimental data from the calibration wind tunnel are used

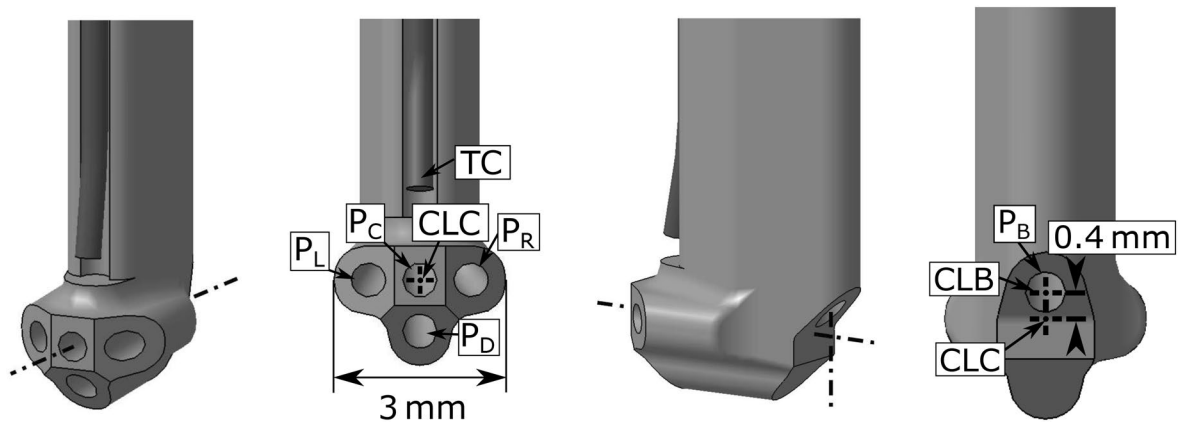


Fig. 2 Probe head of five-hole probe with probe pressures (P_C , P_L , P_R , P_D , P_B), thermocouple (TC) and center lines of center hole (CLC), as well as of base pressure hole (CLB)

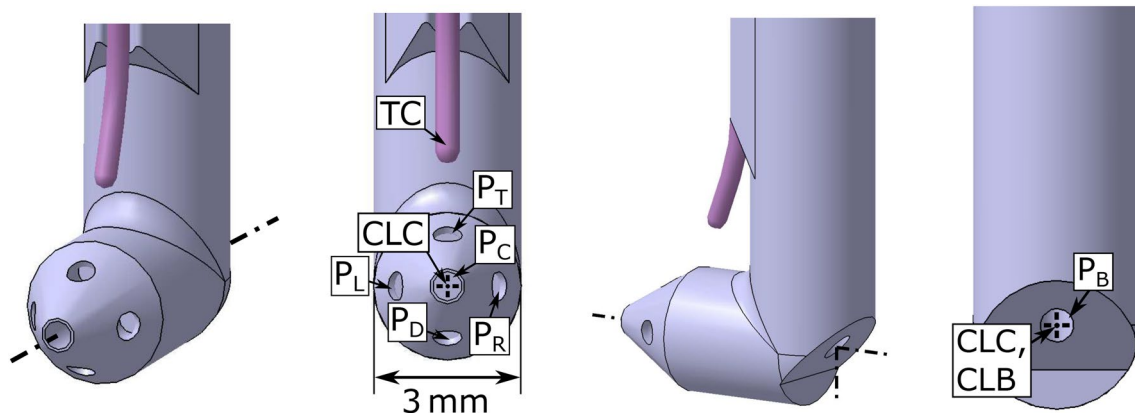


Fig. 3 Probe head of six-hole probe with probe pressures (P_C , P_L , P_R , P_D , P_T , P_B), thermocouple (TC) and center lines of center hole (CLC), as well as of base pressure hole (CLB)

for a comparison of measurement deviations with three different evaluation methods. An approach based on a conventional Mach number determination using front pressures is compared with the method using the base pressure hole and a combination of the two. An analysis which method should be used in transonic flows is performed.

2 Pneumatic probes

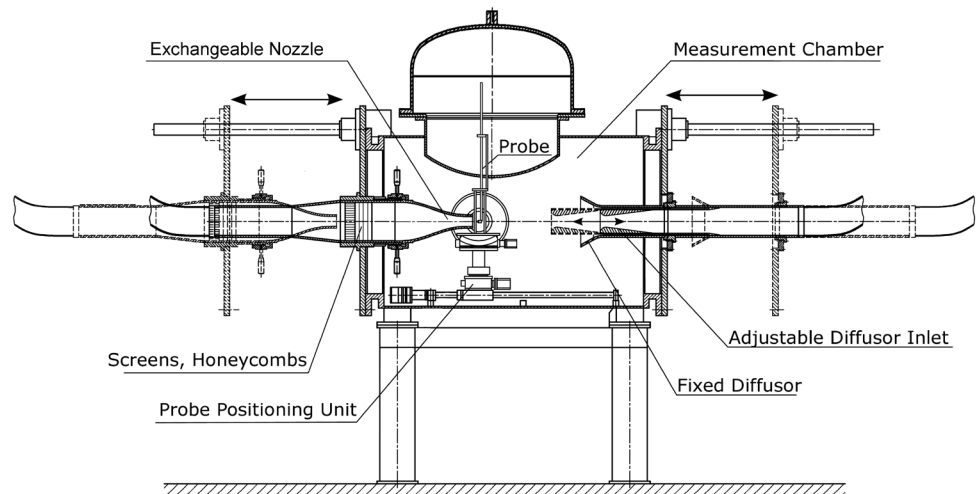
The two probe types considered in the investigation were manufactured by selective laser melting (SLM). The probes were afterwards reworked to ensure clean surfaces and edges at and near the pressure holes. In Figs. 2 and 3, the probe heads are shown. The naming convention for the probe pressures is included. The head diameter is 3 mm for both probes. Each probe has a thermocouple TC that is located above the probe head. For the purpose of determining Mach

numbers, the only temperature-dependent variable is the isentropic coefficient κ , which is calculated from empirical functions.

The pressure holes of the five-hole probe (5HP) are split between the four holes facing forward and the base pressure hole on the back side. The angle between the side planes and the central plane is 45° . Notable are the sharp edges between the plane surfaces containing the pressure holes. These are intended to induce flow separation along defined lines to reduce the Reynolds-sensitivity of the probe. A similar reasoning led to the design of the probes investigated by Kost [9]. However, the opposing view that sharp edges increase the influence of the Reynolds number on probe behavior has also been expressed [13]. In the present study, the Reynolds number during the calibration is matched to the flow conditions during the measurements in a research turbine. Hence, the Reynolds number influence will not be discussed further.

The base pressure hole of the 5HP is also situated behind a sharp edge meant to induce flow separation and prevent the

Fig. 4 Cross-section of SKG calibration wind tunnel test section. Adapted from Fig. 1 in [2]



hole from being directly impinged by the flow if radial flow angles are present. The plane containing the pressure hole is inclined by 45° with respect to the probe head center axis. Moreover, the base pressure hole is placed 0.4 mm above the central pressure hole.

The six-hole probe (6HP) has an additional pressure hole on the top side of its cone-shaped head which is missing in the design of the 5HP. The cone angle is 60° resulting in a sharper head geometry compared to the 5HP. The design around the base pressure hole is similar to the 5HP, also featuring a sharp separation edge. However, the hole is situated on the probe head axis. Thus, both the center hole facing forward and the base pressure hole are at the same radial position if the probe shaft is perpendicular to the machine axis. The 6HP was developed based on the general design of the 5HP. Here, the offset between the center and base pressure holes provides additional safety against impinging flow. However, due to the radial pressure gradients in research turbines, this radial offset is a potential source of errors. To eliminate this effect, the base pressure hole was moved onto the center hole center line in the design of the 6HP.

3 Probe calibration

This section describes the calibration facility and gives a brief overview of the calibration procedure and instrumentation. The comparison between the evaluation methods is influenced by the aerodynamic behavior of the probes and the measurement setup. Consequently, measurement ranges as well as the related accuracies are given for each probe pressure. Moreover, the calibration ranges with respect to flow angles, and Mach and Reynolds numbers are provided.

3.1 Calibration wind tunnel

The calibration was performed at the Probe Calibration Facility (SKG, in previous publications called SEG) at the German Aerospace Center (DLR) in Göttingen. A cross-sectional view of the measurement chamber can be seen in Fig. 4. This closed-loop calibration wind tunnel is designed to independently match Mach and Reynolds numbers to the conditions during the turbomachinery measurements. This is achieved by varying the total pressure in the settling chamber and thus the chamber pressure at a given Mach number. The total temperature is kept at about 293 K. The calibration flow is a free jet with a diameter of 50 mm. To cover a wide range of Mach numbers, the volume flow through the measurement chamber can be varied and different exchangeable nozzles can be installed. Up to $Ma = 0.8$, a convergent subsonic nozzle is used. Transonic calibrations in the range between $Ma = 0.9$ and $Ma = 1.3$ are conducted with a slotted nozzle. A detailed description of the calibration wind tunnel is presented by Gieß [2]. After modifications that have taken place since this publication, Mach numbers from about 0.05 to 1.8 and total pressures from 30 to 150 kPa can be reached. For $Ma \geq 0.2$, a turbulent intensity of 1% was measured with a hot-wire probe. Windows in the measurement chamber provide optical access to the calibration free jet, e.g., for Schlieren or particle image velocimetry (PIV) measurements.

3.1.1 Calibration procedure

For the calibration, the probes are mounted in the probe positioning unit, as depicted in Fig. 5. With its two rotational axes, the probe positioning unit allows automated adjustment of the two flow angles α and β seen in Fig. 6. At the start of the calibration, the probe shaft is brought into an orientation perpendicular to the nozzle. Subsequently, the

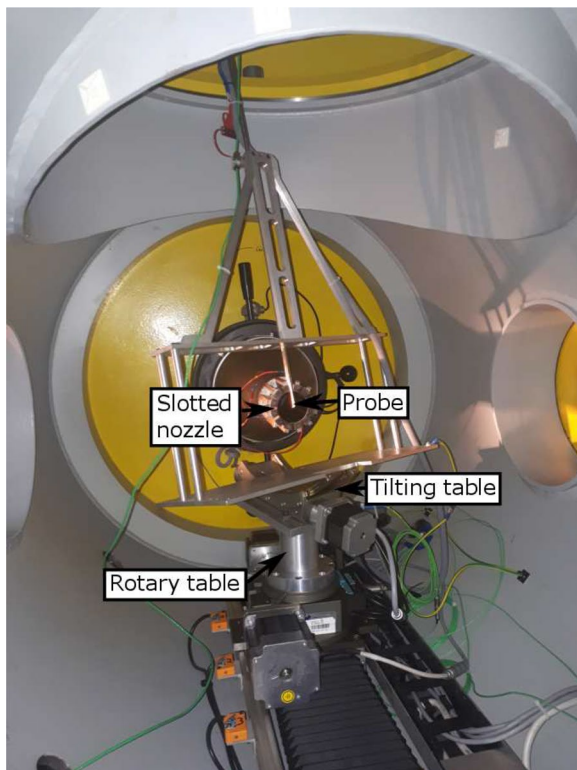


Fig. 5 Probe in calibration wind tunnel

probe is rotated around its shaft until $P_L \approx P_R$. In this orientation, both angles α and β are zero. The accuracy of this initial probe alignment is estimated as $\pm 0.05^\circ$ for α and $\pm 0.12^\circ$ for β . During the alignment and the following calibration, the flow angle α is always approached from one direction to ensure that backlash has no influence on the positioning accuracy. The backlash of the other axis is negligible relative to the accuracy of the alignment with regards to β . The rotational accuracy relative to α , $\beta = 0^\circ$ is $\pm 0.05^\circ$ for α and $\pm 0.1^\circ$ for β .

3.1.2 Instrumentation and data acquisition

The total pressure is measured in the settling chamber upstream of the nozzle with a pitot tube that is connected to a Mensor Precision Pressure Indicator CPG2500 absolute pressure transducer. The same pressure transducer is used for the static pressure that is taken at a wall tap in the measurement chamber. All probe pressures are measured with a Model 9116 Pneumatic Intelligent Pressure Scanner by Pressure Systems. The measurement ranges for different probe pressures depending on the Mach number are listed

in Table 1. The relative static accuracy of the differential pressure measurements is 0.05% of the respective full-scale values [14]. Thus, to optimize the absolute static accuracy, the measurement ranges were chosen according to the expected maximum differential pressure at each pressure hole. The selected configuration provides a good match between the measurement ranges of the available pressure scanners and the maximum differential pressures. The differential pressures are relatively low at the pressure holes on the probe front due to the proximity of these holes to the stagnation point. In contrast, as the probe pressure P_B is close to the static pressure of the flow, its measurement requires a larger measurement range. All differential pressures increase in magnitude with increasing Mach number, necessitating a distinction between calibration in sub- and transonic flow. The relative static accuracy of the absolute pressure measurement is 0.01% of its measurement range of 300 kPa [15]. All accuracy statements given in this section take the combined effects of errors related to linearity, repeatability and hysteresis into account. All pressures are sampled with a mean frequency of 2 Hz over 3 s at each calibration point after a waiting time of 3–5 s during which the pressures equalize.

3.1.3 Calibration ranges

During the actual measurements in research turbines, the probes are inserted through the casing in radial direction, usually perpendicular to the machine axis. The probes can be moved between measurement points in the radial direction and also rotated around their shaft. By means of this rotation, the probe angle α can be minimized, and hence, only a small calibration range is required with respect to α .

On the other hand, the presence of large radial flow angles must be accounted for with a sufficiently large

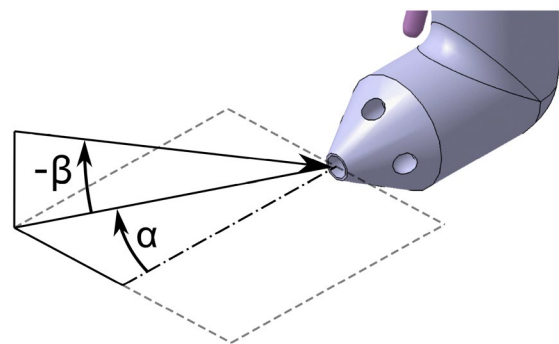


Fig. 6 Flow angles α and β

Table 1 Probe pressure measurement ranges

Mach number	Measurement range [kPa]					
	P_C	P_L	P_R	P_D	P_T	P_B
≤ 0.8	± 34.5	± 68.9	± 68.9	± 68.9	± 68.9	± 206.8
> 0.8	± 68.9	± 68.9	± 68.9	± 68.9	± 206.8	± 206.8

Table 2 Calibration ranges of flow angles

	α	β
5HP	-10° to 10°	-12° to 32°
6HP	-10° to 10°	-22° to 32° (Ma ≤ 0.8) -21° to 32° (Ma > 0.8)

calibration range with regards to the flow angle β , which reaches up to 32° . The calibration ranges for both flow angles are given in Table 2. As the probes are calibrated for use in different experiments, the calibration range with respect to β is smaller for the 5HP. Moreover, the increase in the lower calibration threshold from $\beta = -22^\circ$ to $\beta = -21^\circ$ for the 6HP is necessary to avoid collision with the slotted nozzle used for transonic calibration. The maximum step size between adjacent angles in the calibration grid is 3° for α and 4° for β .

In this study, both probes are calibrated up to $Ma \approx 1.3$ in steps of ≈ 0.1 . For the 6HP, the step size is reduced to ≈ 0.05 for $Ma > 1.2$. The total pressure during calibration is kept constant at 30 kPa to achieve Reynolds number similarity to the experiment. As a result, the Reynolds number using the probe head diameter of 3 mm as the characteristic length remains roughly constant at 12,500 throughout transonic flow.

4 Probe coefficients and interpolation

Dimensionless coefficients are calculated from the probe pressures recorded during the calibration. The coefficients with high angle sensitivity for the 6HP are defined as (see [1])

$$C_\alpha = \frac{P_L - P_R}{P_C - P_{m,6HP}} \tag{1}$$

$$C_\beta = \frac{P_D - P_T}{P_C - P_{m,6HP}} \tag{2}$$

with

$$P_{m,6HP} = \frac{P_L + P_R + P_D + P_T}{4} \tag{3}$$

For the third coefficient, two options will be discussed. Main [8] showed that with the probe pressures on the front side, a pseudo-Mach number

$$C_{Ma} = \sqrt{\frac{2}{\kappa - 1} \left[\left(\frac{P_{m,6HP}}{P_C} \right)^{\frac{1-\kappa}{\kappa}} - 1 \right]} \tag{4}$$

can be calculated that has a nearly linear relation to the actual Mach number in subsonic flow.

As the slope $m(C_{Ma}) = \frac{\partial C_{Ma}}{\partial Ma}$ is reduced significantly or may even vanish completely near $Ma = 1$, Kost [9] proposed the alternative coefficient

$$C_{Mab} = \sqrt{\frac{2}{\kappa - 1} \left[\left(\frac{P_B}{P_C} \right)^{\frac{1-\kappa}{\kappa}} - 1 \right]} \tag{5}$$

The base pressure from the back side of the probe replaces the mean over pressures from the probe front side as the indicator of static pressure. As discussed in the introduction, this coefficient is meant to avoid the Mach number insensitivity in transonic flow.

Due to the 5HP missing the probe pressure P_T , the coefficients are modified slightly for this probe with the alternative definition

$$P_{m,5HP} = \frac{P_L + P_R}{2} \tag{6}$$

replacing $P_{m,6HP}$ in Eqs. 1, 2 and 4. Additionally, P_C replaces P_T in formula 2, leading to

$$C_\beta = \frac{P_D - P_C}{P_C - P_{m,5HP}} \tag{7}$$

As, during the calibration, the flow conditions are known, the calibration data contain the relationship between the coefficients and the flow parameters, e.g., Ma . During the measurement in an unknown flow, these parameters can thus be interpolated from the calibration data. For this purpose, a local linear interpolation based on multiple coefficients is performed. For accurate measurements in three-dimensional flow, at least two angle coefficients, C_α and C_β , and one Mach number coefficient, C_{Ma} or C_{Mab} , must be used. This ensures that for each flow parameter influencing the probe behavior, there is one coefficient with high sensitivity. However, there

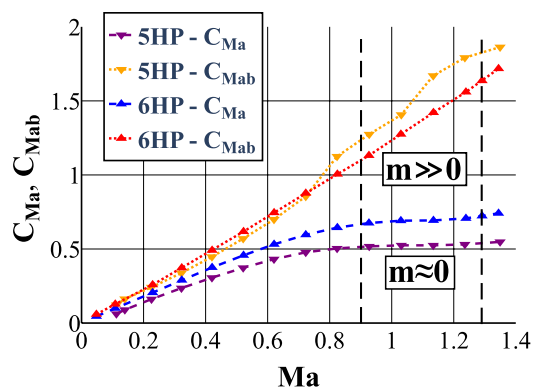


Fig. 7 Calibration coefficients C_{Ma} and C_{Mab} for $\alpha, \beta = 0^\circ$ and slope m in transonic flow

is no limit to the number of coefficients used and a higher dimensional interpolation is possible, as well.

5 Results and discussion

This section contains a presentation of the calibration data for both probes and the determination of measurement deviations with the 6HP. First, the probe behavior at zero incidence, i.e., $\alpha, \beta = 0^\circ$, is considered. This allows a comparison to the probe behavior reported by Kost [9]. The influence of radial flow angles on the Mach number coefficients is investigated with calibration data at different values of β . Finally, a comparison of measurement deviations is conducted for the 6HP. This includes a comparison of different evaluation methods.

5.1 Probe behavior at zero incidence

The curves of the coefficients C_{Ma} and C_{Mab} for $\alpha, \beta = 0^\circ$ are depicted in Fig. 7. To maximize the measurement accuracy, the following requirements should be fulfilled:

- **High sensitivity:** The slopes $m(C_{Ma}) = \frac{\partial C_{Ma}}{\partial Ma}$ and accordingly $m(C_{Mab}) = \frac{\partial C_{Mab}}{\partial Ma}$ can be regarded as measures of the sensitivity of the coefficients regarding the Mach number. Kost [9] and Börner et al. [11] showed that greater slopes lessen the impact of a given pressure error on the resulting Mach number.
- **Good linearity,** i.e., a constant slope: The magnitude of interpolation errors depends on how well the model functions conform to the probe behavior. Therefore, linear probe behavior is especially desirable if linear interpolations are used. Regardless of the exact interpolation method, achieving a smooth probe behavior without strong local effects reduces interpolation errors. Most

importantly, a biunique relation between the coefficient and the Mach number must exist, i.e., every value of the coefficient must correspond to exactly one value of the Mach number and vice versa. Hence, the slope must always remain positive.

Starting from approximately $Ma = 0.8$, the decrease of the slope $m(C_{Ma})$ becomes evident for both probes. Between $Ma = 1$ and $Ma = 1.1$, it becomes negligibly small. Conversely, a slight increase in $m(C_{Ma})$ can be seen for $Ma > 1.2$. The reason for the beginning of the insensitivity has already been discussed. On the other hand, a reemergence of the probe sensitivity at increasing Mach numbers is visible. According to Kost [9] and Humm [16], this is a consequence of the transition from a detached, approximately normal shock to an oblique shock that is attached to the probe tip. In contrast to the normal shock, the oblique shock does not lead to a reduction of the downstream Mach number below unity. As a result, a supersonic flow region is present in the vicinity of the front pressure holes. Thus, the dependence of the pressure near the probe head tip on the Mach number is restored.

However, according to Shapiro [17], flow attachment for a cone angle of 60° , equivalent to the design of the probe head of the 6HP, occurs at $Ma \approx 1.5$. For the blunter 5HP with a larger included angle at the probe head, flow attachment should be delayed to even higher Mach numbers. Hence, the occurrence of attached shocks at $Ma < 1.3$ is unlikely for both probes. Thus, the increasing curvature of the shock at increasing Mach numbers could be sufficient to cause the observed reemergence of sensitivity.

In contrast, the alternative coefficient C_{Mab} retains its positive slope throughout the investigated Mach number range for both probe types. The curve of the six-hole probe exhibits better linearity, while the maximum value and, thus, the mean slope over the whole calibration domain are slightly higher for the 5HP.

5.2 Flow angle variation

When defining dimensionless pressure coefficients, it is desirable to achieve high sensitivity with regards to one flow property and low sensitivity with respect to all other properties. The reason for normalizing the pressure difference over the side pressures with the term $P_c - P_m$ in Eqs. 1, 2 and 7 is to decrease the influence of the Mach number on the coefficients C_α and C_β [18]. As a result, interpolation errors are reduced. Accordingly, a probe should be designed in such a way that the coefficients C_{Ma} and C_{Mab} are independent of the flow angles. Due to the possibility of rough alignment of the probes in the α -direction, the influence of β is of primary concern for turbomachinery measurements.

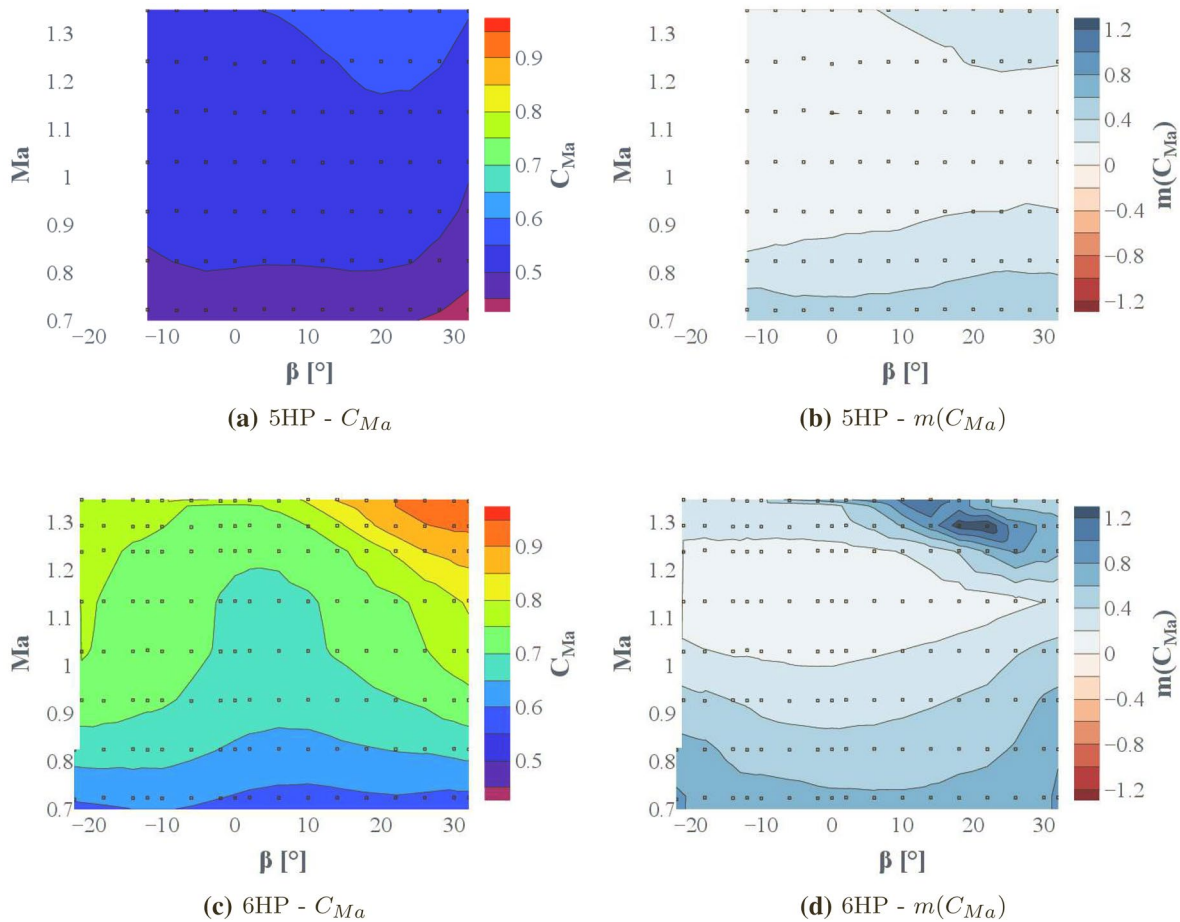


Fig. 8 Values and slopes of C_{Ma} for 5HP (a, b) and 6HP (c, d)

The maps of the coefficient C_{Ma} at $\alpha = 0^\circ$ depending on Mach number and flow angle β are shown in Fig. 8. Calibration points are indicated with dots. While there is some dependence on β for both probes in Fig. 8a, c, it is much more pronounced for the 6HP. To highlight differences in local probe behavior, the difference quotient, equivalent to the slope m for the piecewise calibration function, is calculated from

$$m(C_{Ma}) = \frac{C_{Ma}[p_1] - C_{Ma}[p_2]}{Ma[p_1] - Ma[p_2]}. \tag{8}$$

Here, p_1 is the evaluated calibration point and p_2 is its closest neighbor at a lower Mach number and constant flow angle β .

As can be seen by comparing Fig. 8b with 8d, the insensitivity stretches over a wider range of Mach numbers for the 5HP. In contrast, for the 6HP the region with the smallest slope shrinks down to the interval between $Ma \approx 1$ and $Ma \approx 1.2$, especially for large positive values of β . There appears to be some influence of the probe shaft or perhaps geometrical irregularities related to the manufacturing process which

cause slight asymmetries with respect to β for both probes. Hence, for the 6HP, the region with the most severe insensitivity appears to be roughly between $\beta = -15^\circ$ and $\beta = 10^\circ$.

The difference between the probe types is in line with the aforementioned relation between the sensitivity of a probe and the shape of the bow shock. The sharper probe head of the 6HP results in a more curved shock with a smaller standoff distance and an overall smaller subsonic region. The reason for the increase in sensitivity at high incidence is not yet fully understood. However, in this case, some of the pressure holes may at least partially fall outside the subsonic region, thereby increasing $m(C_{Ma})$.

The alternative coefficient C_{Mab} and its slope $m(C_{Mab})$ are depicted in Fig. 9. The color scale for $m(C_{Mab})$ is cut at 1.2 to highlight zones with low sensitivity. For the 5HP, $m(C_{Mab})$ is lowest for large angles β between $Ma = 1$ and $Ma = 1.2$ (see Fig. 9b). Neither the influence of β nor of the Mach number can be eliminated using C_{Mab} instead of C_{Ma} . Still, $m(C_{Mab})$ is greater than $m(C_{Ma})$ with exceptions occurring only in small regions of the calibration domain.

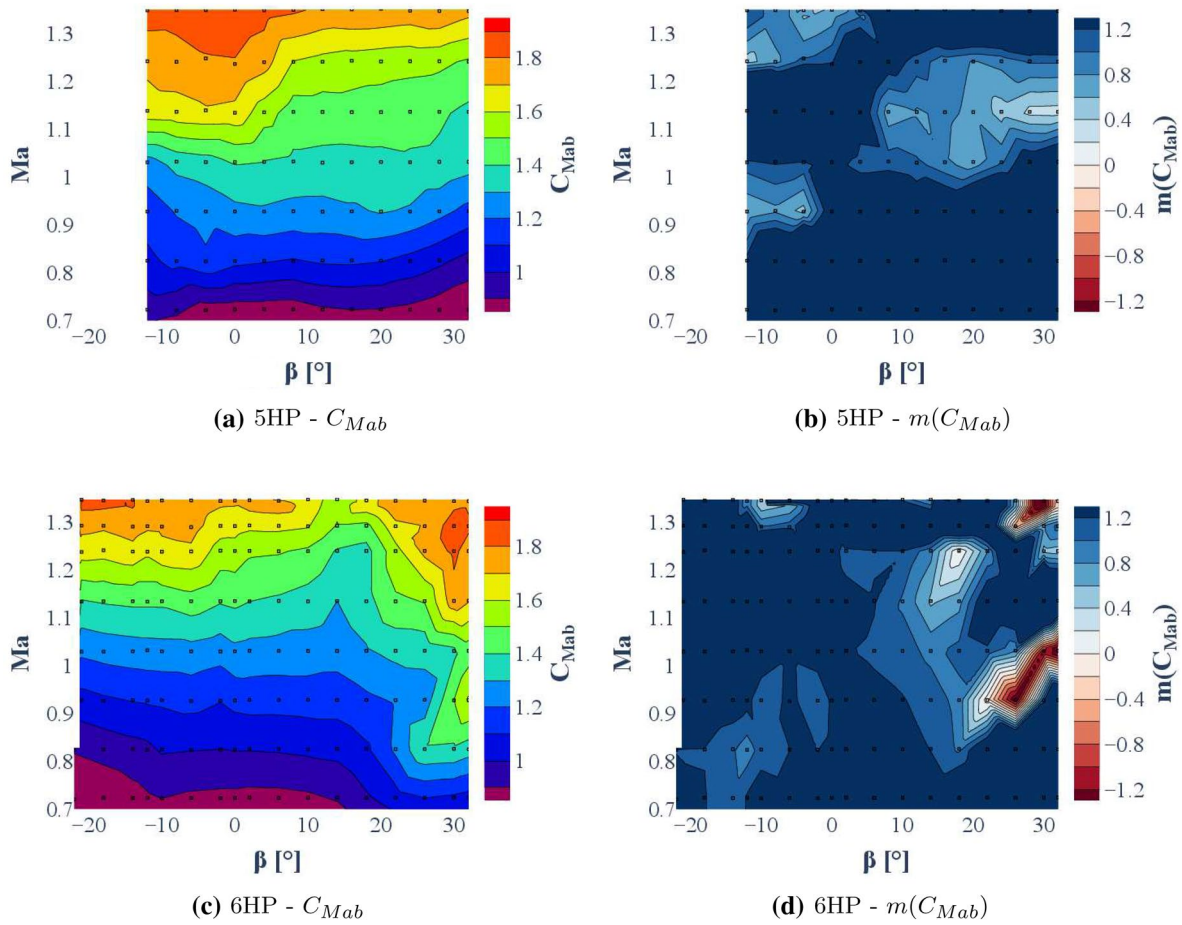


Fig. 9 Values and slopes of C_{Mab} for 5HP (a, b) and 6HP (c, d)

The behavior of C_{Mab} for the 6HP at high positive angles β is more complex (see Fig. 9c). Starting between $\beta = 22^\circ$ and $\beta = 26^\circ$, negative values of $m(C_{Mab})$ occur (see Fig. 9d). Therefore, the relationship between the coefficient and the Mach number is not biunique for a given angle β in these regions. For example, at $\beta = 26^\circ$, the value of C_{Mab} at $Ma = 0.8$ is about the same as at $Ma = 1.0$ with a smaller value in between. Consequently, based on the coefficient, it is not possible to differentiate between the two Mach numbers.

It is possible that for large positive flow angles β , the flow impinges directly on the base pressure hole. In this case, the base pressure P_B is not only affected by the static pressure in the far field but senses part of the dynamic pressure. As a consequence, the value of C_{Mab} is reduced.

The difference in probe behavior is most likely related to the design of the separation edge on the back side of the

probes. The fact that, for the five-hole probe, the base pressure is placed slightly above the center line of the center

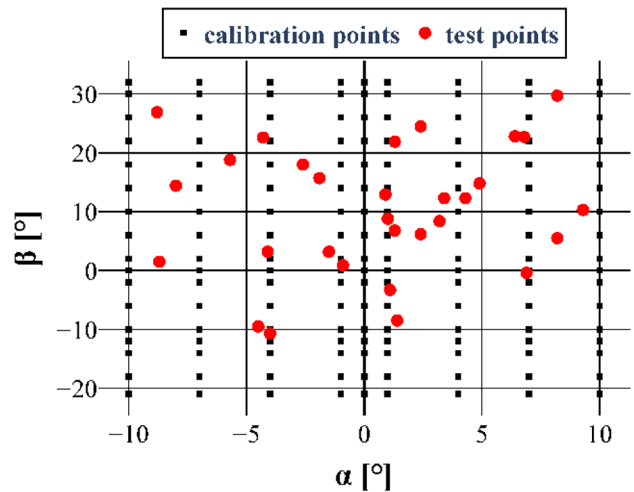


Fig. 10 Distribution of calibration points and test points

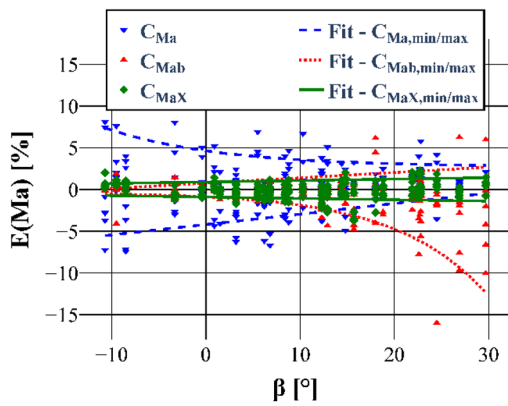


Fig. 11 $E(Ma)$ for different evaluation methods

pressure hole may also have an effect. Thus, the calibration data point towards a possible trade-off. On the one hand, placing the base pressure further from the separation edge could prevent flow impingement up to higher radial flow angles. On the other hand, this may introduce measurement errors if strong radial pressure gradients are present during the turbomachinery measurement.

5.3 Measurement deviations

The fact that the relationship between C_{Mab} and the Mach number is not biunique is expected to have a detrimental effect on the measurement accuracy. Therefore, additional data on the performance of the 6HP were collected. These were acquired by measuring the probe pressures at test points that are not part of the calibration data. The measurements were conducted at the calibration wind tunnel SKG. Hence, the reference Mach number Ma_{ref} is known and the difference

$$E(Ma) = \frac{Ma_{probe} - Ma_{ref}}{Ma_{ref}} \tag{9}$$

between the measurement result Ma_{probe} based on interpolation and based on Ma_{ref} can be determined. This is the measurement deviation¹ of the probe in the homogeneous calibration flow.

For Ma_{probe} , not only the results from three-dimensional interpolations with C_{Ma} or C_{Mab} are considered but additionally a four-dimensional interpolation with both coefficients, denoted by C_{MaX} .

The distribution of test points and calibration points with respect to the angles α and β can be seen in Fig. 10. The 30 test points at each Mach number were generated with a random number generator in the intervals $-10^\circ < \alpha < 10^\circ$

and $-12^\circ < \beta < 32^\circ$, respectively. Based on the calibration data, it is likely that the probe behavior over the intervals $-22^\circ < \beta < -12^\circ$ and $-12^\circ < \beta < 10^\circ$ is similar. Therefore, no test points were distributed in the range $-22^\circ < \beta < -12^\circ$. The investigation is limited to transonic flow with $Ma > 0.9$.

The sampling of the test points was repeated at different Mach numbers from 0.95 to 1.25 in steps of 0.05, resulting in 210 points in total. For the calibration data, a grid spacing of 0.1 was selected with respect to the Mach number. To achieve this, the calibration data from Mach number 1.25 were neglected, resulting in an equidistant calibration grid that is more representative of the usual procedure when calibrating probes. Thus, 90 of the test points were recorded at Mach numbers coinciding with the calibration grid and 120 points are located halfway between the values of the calibration grid.

Consequently, multiple factors leading to measurement errors are considered:

- Slope of the coefficients
- Accuracy of pressure measurements
- Interpolation errors from nonlinear probe behavior.

The resulting measurement deviations for all 210 test points are shown in Fig. 11 against β . To visualize the general trends, fit functions were generated based on the largest deviations in positive and negative direction for each value of β . There is a nearly linear decrease of the maximum and minimum deviations using C_{Ma} with increasing angle β which is coinciding with the increase of $m(C_{Ma})$ in Fig. 8. In contrast, the absolute values of $E(Ma)$ using C_{Mab} increase for larger angles β , which is also in line with the development of $m(C_{Mab})$ in Fig. 9. These contrary effects result in a strong reduction of the influence of the flow angle β on the measurement deviations in the case of C_{MaX} .

To give a more complete impression of the distribution of $E(Ma)$, histograms of relative frequency are shown in Fig. 12. For the 98 points with $\beta \leq 10^\circ$, C_{Mab} leads to a much narrower dispersion and is thus clearly preferable over C_{Ma} (see Fig. 12a). However, for the 112 points with $\beta > 10^\circ$, the maximum absolute values of $E(Ma)$ occur for C_{Mab} (see Fig. 12b). The measurement deviation $E(Ma)$ using C_{Mab} reaches -16% at a single point, which exceeds the displayed range. In contrast, C_{MaX} results in the distributions with the narrowest dispersions in both histograms with partial data as well as the overall view in Fig. 12c.

These impressions are reinforced by the quantitative assessment of the sample standard deviations $\sigma(E(Ma))$ in Table 3 and the maximum absolute deviations $|E(Ma)|_{max}$ in Table 4. For flow angles $\beta \leq 10^\circ$, there is a clear reduction of $\sigma(E(Ma))$ of about 75% if the interpolation is based on

¹ Measurement deviation = “measurement value minus a reference value” [19].

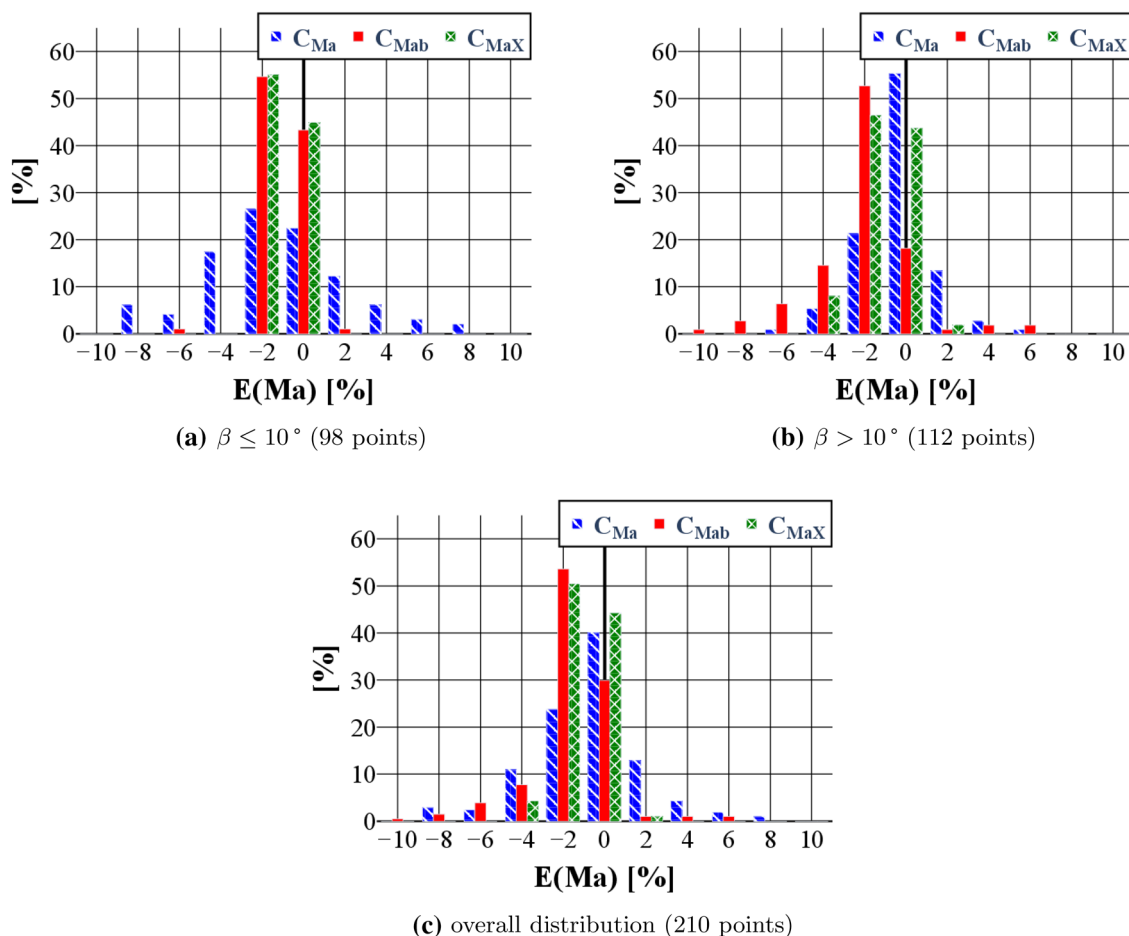


Fig. 12 Distribution of $E(Ma)$ for 6HP with different evaluation methods and ranges of β

Table 3 Sample standard deviations $\sigma(E(Ma))$ in [%]

	Overall	$\beta \leq 10^\circ$	$\beta > 10^\circ$
C_{Ma}	2.7	3.4	1.8
C_{Mab}	2.2	0.8	2.8
C_{MaX}	0.9	0.7	1.1

Table 4 Maximum measurement deviations $|E(Ma)|_{max}$ in [%]

	$\beta \leq 10^\circ$	$\beta > 10^\circ$
C_{Ma}	8.1	6.7
C_{Mab}	4.1	16
C_{MaX}	2	3.7

C_{Mab} instead of C_{Ma} . However, in the interval $\beta > 10^\circ$, the same approach leads to an increase of $\sigma(E(Ma))$ by about 55% compared to the evaluation based on C_{Ma} . If all 210 test points are considered, the differences between the two three-dimensional interpolations are relatively minor, especially with regards to $\sigma(E(Ma))$. In contrast, using both coefficients

simultaneously reduces the sample standard deviation by more than 50% compared to C_{Mab} and 66% compared to C_{Ma} . The maximum absolute values of the deviation are also reduced substantially.

6 Conclusions and outlook

1. A five-hole probe and a six-hole probe with a special base pressure hole for transonic Mach measurements were calibrated for radial flow angles up to 32° and Mach numbers up to 1.3. As suggested by Kost [9], a dimensionless calibration coefficient can be defined with the base pressure that does not exhibit the insensitivity of common probe designs in transonic flow.
2. For the six-hole probe with a cone-shaped head, the insensitivity of the coefficient with pressures from the probe front side affects a slightly narrower band of Mach numbers compared to the blunter five-hole probe. For both probes, an increase in sensitivity was observed with

an increase in radial flow angle. However, the effect is stronger for the six-hole probe.

3. For both probes, the Mach number coefficient using the base pressure has a higher sensitivity compared to the Mach number coefficient using only pressures from the probe front. For the five-hole probe, a decrease in sensitivity was observed in parts the calibration domain mainly at large flow angles. However, these parts were small as only few calibration points were affected. In contrast, for the six-hole probe, the relationship between the coefficient and the Mach number is not biunique at radial flow angles exceeding 22° . The difference in probe behavior is likely connected to the geometry of the separation edge and placement of the base pressure hole.
4. The influence of the aerodynamic behavior and evaluation method on measurement results was examined for the six-hole probe by comparing the interpolated results at 210 randomly distributed points with reference values. In this manner, the combined influence of pressure measurements, calibration coefficients, and interpolation errors were examined. Using the coefficient calculated with the base pressure results in a clear reduction of measurement deviations for radial flow angles up to 10° compared to the coefficient with front side pressures. The sample standard deviation over 98 points was reduced by 75%. In contrast, for larger radial flow angles from 10° to 32° , an increase of sample standard deviation by more than 50% was observed with this method. The lowest deviations, irrespective of the radial flow angle, were achieved with an interpolation using both Mach number coefficients. Considering all 210 points, the empirical standard deviations were reduced by more than 50% and 66% compared to interpolations with only the base pressure coefficient and the conventional coefficient, respectively. As the study focused purely on the determination of the Mach number, further investigations are necessary concerning the influence on other quantities such as flow angles, total temperature, and total pressure. Moreover, additional data are necessary to decide if the approach is also advantageous for the five-hole probe. Compared to the six-hole probe, this probe has lower Mach number sensitivity if the front pressures are used which could decrease the effectiveness of the four-dimensional interpolation. Still, the proposed method appears to have great potential in improving the accuracy of transonic probe measurements.
5. In conclusion, the results emphasize the necessity for further studies concerning the design of probes for measurements in transonic flows with high radial flow angles. The present study focuses on differences in the aerodynamic behavior between two single probes of different designs. However, one of the reasons experimental calibrations are performed is the influence of manu-

facturing-related geometrical irregularities on the probe behavior. Based on the calibration data of a larger number of probes, it should be assessed if such irregularities can fundamentally alter the probe behavior such as the occurrence of vanishing slopes of coefficients. If the impact of geometric irregularities is only minor, further optimization of probe geometries could benefit from the performance of numerical calibrations of probe models by means of computational fluid dynamics. These could help to reduce the number of experimental investigations of new probe designs and thus to speed up the development process. The suitability of this approach should be the subject of additional research.

Acknowledgements The probe calibrations were performed with partner Rolls Royce Germany within the Project HittTurb as well as with partner Siemens Energy within the Project Rotating Turbine Rig. The authors would like to thank Siemens Energy for assisting in the development of the six-hole probe investigated in this study.

Funding Open Access funding enabled and organized by Projekt DEAL.

Declarations

Conflict of interest The authors declare that they have no conflicts of interest.

Open Access This article is licensed under a Creative Commons Attribution 4.0 International License, which permits use, sharing, adaptation, distribution and reproduction in any medium or format, as long as you give appropriate credit to the original author(s) and the source, provide a link to the Creative Commons licence, and indicate if changes were made. The images or other third party material in this article are included in the article's Creative Commons licence, unless indicated otherwise in a credit line to the material. If material is not included in the article's Creative Commons licence and your intended use is not permitted by statutory regulation or exceeds the permitted use, you will need to obtain permission directly from the copyright holder. To view a copy of this licence, visit <http://creativecommons.org/licenses/by/4.0/>.

References

1. Treaster, A.L., Yocum, A.M.: The calibration and application of five-hole probes. Technical report TM 78-10, Pennsylvania State University, Institute for Science and Engineering, Applied Research Laboratory, Pennsylvania, USA (1978)
2. Gieß, P.A., Rehder, H.J., Kost, F.: A new test facility for probe calibration-offering independent variation of Mach and Reynolds number. In: 15th Symp. on Meas. Tech. in Transonic and Supersonic Flow in Cascades and Turbomach., Florence, Italy, Sep. 21–22, (2000)
3. Hölle, M., et al.: Measurement uncertainty analysis for combined multi-hole pressure probes with a temperature sensor. In: Int. Gas Turbine Congr., Nov. 15–20, Tokyo, Japan, pp. 1527–1538 (2015)
4. Fransson, T.H., Schulz, K., Schaller, F.: Change of flow conditions due to the Introduction of an aerodynamic probe during calibration. In: 9th Symp. on Meas. Tech. for Transonic and Supersonic

- Flows in Cascades and Turbomach, Mar 21–22, Oxford, UK (1988)
5. Sinclair, J., Cui, X.: A theoretical approximation of the shock standoff distance for supersonic flows around a circular cylinder. *Phys. Fluids* **29**(2), 026102 (2017). <https://doi.org/10.1063/1.4975983>
 6. Mishra, A., Khan, A., Musfirah Mazlan, N.: Determination of shock standoff distance for wedge at supersonic flow. *Int. J. Eng.* **32**(7), 1049–1056 (2019). <https://doi.org/10.5829/ije.2019.32.07a.19>
 7. Hancock, P.E.: A Theoretical constraint at $M = 1$ for intrusive probes and some transonic calibrations of simple static-pressure and flow-direction probes, In: 9th Symp. on Meas. Tech. in Transonic and Supersonic Flow in Cascades and Turbomach. Mar 21–22, Oxford, UK (1988)
 8. Main, A.J., Day, C.R.B., Lock, G.D., Oldfield, M.L.G.: Calibration of a four-hole pyramid probe and area traverse measurements in a short-duration transonic turbine cascade tunnel. *Exp. Fluids* **21**(4), pp. 302–311 (1996). <https://doi.org/10.1007/s001090000086>
 9. Kost, F.: The behavior of probes in transonic flow fields of turbomachinery. In: 8th Eur. Conf. on Turbomach. (ETC), Graz, Austria, Mar 23–27 (2009)
 10. Börner, M., Niehuis, R.: Development of an additive manufactured miniaturized wedge probe optimized for 2D transonic wake flow measurements. In: 24th Symp. on Meas. Tech. in Transonic and Supersonic Flow in Cascades and Turbomach. Prague, Czech Republic, Aug 29–31 (2018)
 11. Börner, M., Bitter, M., Niehuis, R.: On the challenge of five-hole-probe measurements at high subsonic Mach numbers in the wake of transonic turbine cascades, In: Glob. Power and Propuls. Forum, Montreal, Canada, May 7–9 (2018)
 12. Amecke, J.: Aufbau und Eichung einer neuentwickelten Keilsonde für ebene Nachlaufmessungen, insbesondere im transsonischen Geschwindigkeitsbereich: (neue Ausführung der Sonde). Aerodynamische Versuchsanstalt (AVA), Göttingen, Germany (1968)
 13. Bohn, D.: Untersuchung zweier verschiedener axialer Überschallverdichterstufen unter besonderer Berücksichtigung der Wechselwirkungen zwischen Lauf- und Leitrad. Ph.D. dissertation, RWTH Aachen, Aachen, Germany (1977)
 14. Specialties, Measurement: Ethernet Intelligent Pressure Scanner—NetScannerTM. Data sheet, Hampton, USA (2009)
 15. Mensor, L.P.: Precision pressure indicator CPG2500—Operating instructions. User manual, San Marcos, USA (2021)
 16. Humm, H.J.: Optimierung der Sondengestalt für aerodynamische Messungen in hochgradig fluktuierenden Strömungen. Ph.D. dissertation, ETH Zurich, Zurich (1996)
 17. Shapiro, A.H.: The dynamics and thermodynamics of compressible fluid flow: In two volumes, vol. II., Krieger Publishing, Malabar (1983)
 18. Dudzinski, T.J., Krause, L.N.: Flow-direction measurement with fixed-position probes. National Aeronautics and Space Administration, Cleveland (1969)
 19. Brinkmann, B., DIN e.V.: Internationales Wörterbuch der Metrologie: Grundlegende und allgemeine Begriffe und zugeordnete Benennungen (VIM) Deutsch-englische Fassung ISO/IEC-Leitfaden 99:2007. Beuth Verlag, Berlin (2012)

Publisher's Note Springer Nature remains neutral with regard to jurisdictional claims in published maps and institutional affiliations.